KEK Preprint 95-79
June 1995
A

Nonlinear Resonances in a Multi-Stage Free-Electron Laser

S. HASHIMOTO, K. TAKAYAMA

CERN LIBRARIES, GENEVA
SCAN-9507146

SW9530

Submitted to "Physics Letters A"

National Laboratory for High Energy Physics, 1995

KEK Reports are available from:

Technical Information & Library
National Laboratory for High Energy Physics
1-1 Oho, Tsukuba-shi
Ibaraki-ken, 305
JAPAN

Phone: 0298-64-5136
Telex: 3652-534 (Domestic)
(0)3652-534 (International)
Fax: 0298-64-4604
Cable: KEK OHO
E-mail: Library@kekvax.kek.jp (Internet Address)

Nonlinear resonances in a multi-stage free-electron laser

Satoshi Hashimoto

Department of Accelerator Science, The Graduate University for Advanced Studies,
1-1 Oho, Tsukuba-shi, Ibaraki-ken, 305 Japan

E-mail: hashi@kekvax.kek.jp

Ken Takayama

National Laboratory for High Energy Physics (KEK),
1-1 Oho, Tsukuba-shi, Ibaraki-ken, 305 Japan

ABSTRACT

Significance of nonlinear resonances in a multi-stage free-electron laser for a two-beam accelerator is discussed. A large scale primary resonance observed in numerical simulations is analyzed with a newly developed theoretical model based on both the isolated resonance theory and the macroparticle model.

1. Introduction

A two-beam accelerator (TBA) is a possible candidate for future linear colliders, in which microwave (μ) power required for a high-gradient linac is provided from a multi-stage free-electron laser (MFEL) [1,2] driven by co-propagating, intense, and relatively low-energy electron beam as seen in Fig. 1. Actually, μ-FELs have been experimentally demonstrated in a single stage with notable output power exceeding 1 GW for Ka-band [3] and 100 MW for X-band [4]. In the MFEL, after amplification of input seed-power the driving beam is reaccelerated with an induction unit for energy replenishment to go to the succeeding stage. The TBA driven by a few of multi-stage μ-sources will promise a big advantage of high total efficiency over a conventional linac powered by thousands of klystrons.

One of important beam physics issues in the MFEL is nonlinear resonances (NRs). Murray and Lieberman (M.L.) [5] have presented a theoretical study and simulations on the NR induced in the synchrotron motion due to the periodicity of the MFEL. They have showed that longitudinal dynamics of particles is approximately described in the form of a simple pendulum equation with periodic perturbations and that these resonances, which are identified as bounded and localized resonance islands in the longitudinal phase space, slightly modulate the amplitude and phase of the generated μ. Undoubtedly the TBA/FEL performance strongly depends on a magnitude of such modulation. It was on the early version of TBA/FEL [1] that M.L. have developed their theory, where a fraction of amplified power is extracted by a kind of μ-septum in a steady-state manner [6] and a large amount of power is stored in the waveguide through all stages. The ponderomotive force to give longitudinal focusing is almost constant along the beam pass. The NR originates from mainly the relatively small periodic-variation in the particle energy; loss in FELs and gain at induction units. Unfortunately the early version has been discarded because of practical reasons that the μ-septum is subject to μ-breakdown and μ-transport through the induction gap is subject to reflection and mode conversion.

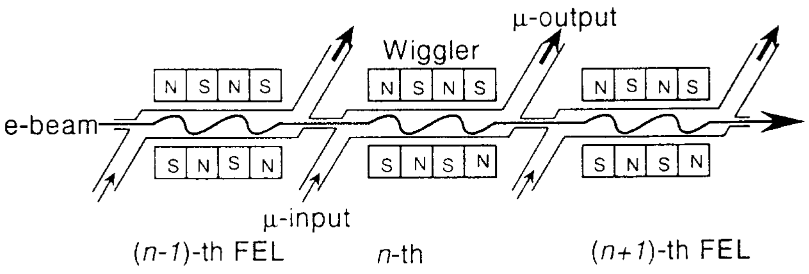

Fig. 1 Schematic view of the multi-stage free-electron laser (the new version of the TBA/FEL).

Recently a different sort of the MFEL has been introduced to remove the above difficulties [2]. In this second version, a small μ power is fed at the start of each stage and all of the amplified power is extracted by an output μ-coupler [4] at the end of the stage. This μ-handling process is distinguished from that of the early version; the ponderomotive forces drastically change through stage. Therefore the M.L.'s theory can't be applied to this case. The dynamical system with such a large periodic modulation is subject to more serious NR. To our knowledge, there has been no theoretical and numerical works which focus on the NR in the second version attracting big concerns of the high-energy accelerator society. In this paper, essential aspects of the NR in the recent version of the MFEL will be manifested by means of so-called multiparticle FEL simulations and a theory of a *nonlinear pendulum* based on both the macroparticle model of the MFEL [7,8,9] and the isolated resonance theory [10]. The primary NRs observed in the simulation will be analyzed by this *nonlinear pendulum* model with periodically and rapidly time-varying "mass".

Future linear colliders demand high-power μ with good quality. For instance, a shot-to-shot jitter in μ's phase and amplitude must be maintained within a tolerable level from a requirement for the final focusing in a collider [8]. A significant obstacle against the quality is amplification of undesired modes in the MFEL. Fortunately the amplification of higher modes can be avoided by suitable choice of the waveguide size, because the FEL resonance energies for undesired higher-order modes shift away from that for the fundamental mode (rectangular waveguide TE_{01} mode) with reducing its size. However we have to pay our attention on the significant side-effect caused by reducing the waveguide size, i.e., the high power-density. The MFEL with the reduced waveguide has an inherent problem; the high power-density leads to the quickly increasing ponderomotive force which is likely to give rise to strong NRs. In a practical sense, it seems to be quite important to develop the NR theory in the MFEL which enables us to choose an optimum waveguide size so as to avoid both the NRs and higher-mode evolution in a realistic MFEL.

2. 1-D FEL simulation

For the 1-D FEL simulations, the standard FEL equations [11,12] are numerically integrated by the Runge–Kutta–Gill method, assuming a single TE_{01} mode. A set of typical parameters of the MFEL of interest is listed in Table 1. In the simulations, an initially bunched beam with a half phase spread of $\Delta\psi = 45^\circ$ and an energy spread of $\Delta\gamma = 1$ is injected in the first stage. Here γ and $\psi = \int (k_w + k_s) dz - \omega_s t + \varphi_s$ are the Lorentz factor and ponderomotive phase of a particle, ω_s is μ's angular frequency, k_w the wavenumber of wiggler, a^* the horizontal size of rectangular waveguide,

$k_s = \sqrt{(\omega_s/c)^2 - (\pi/a^*)^2}$ the wavenumber for TE$_{01}$ mode, φ_s the signal phase, t time, z longitudinal coordinate, and c the speed of light. Particles outside an rf bucket don't coherently lose their energy owing to the FEL interaction but periodically gain the energy by repetitive passage through induction units. In the simulations, hence, particles exceeding a typical limit ($\gamma > 30$) in such a manner are removed from the calculation, because high energy particles are not matched to the beam-transport line designed for the resonant energy of the FEL.

Table 1. TBA/FEL parameters

beam current	I	2 kA
beam energy (Lorentz factor)	γ	23
energy gain per period	$\Delta\gamma$	1
wiggler wave length	λ_w	26 cm
wiggler length per period	L_w	52 cm
wiggler peak field	B_w	3.85-3.6 kG
signal frequency	f_S	17.1 GHz
input power	P_{in}	10 MW
waveguide width	a^*	20–4 cm
waveguide height	b^*	3 cm
number of FEL stage		300

In order to evaluate effects of the μ power-density on the NRs, only the waveguide width a^* is varied while the other parameters are fixed. This never alters the FEL resonance condition for TE$_{01}$ mode, because the phase velocity of TE$_{01}$ mode dose not depend on a^*. For a relatively wide waveguide ($a^* \geq 10$ cm), our simulation shows that the beam propagates from the first to the 300-th stage without particle loss, maintaining the original bunch shape. This is just the result which was obtained in the previous simulation [8]. For cases of smaller waveguide $a^* = 8$, 4 cm, meanwhile, the fourth and third-integer resonances are observed in an extremely large-scale, as shown in Figs. 2(a) and (b). These resonances are understood to be caused by the strong μ fields resulting from the reduced waveguide width. The phase-space structure in the MFEL longitudinal dynamics has been found to strongly depend on the waveguide dimension, that is, the μ power-density.

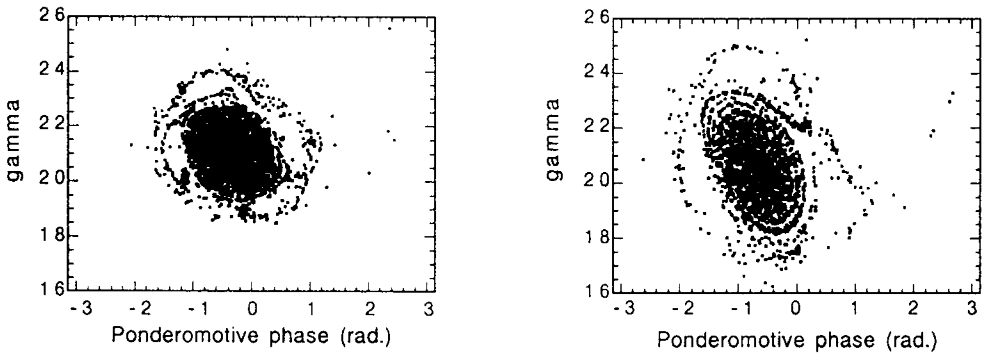

(a) (b)

Fig. 2 Longitudinal phase-space structure for the FEL simulation. (a) the fourth-integer resonance ($a^* = 8$ cm). (b) the third-integer resonance ($a^* = 4$ cm).

Typical degradation of the MFEL performance are shown in Figs. 3(a), (b) where the power and phase of the generated μ are plotted as functions of FEL stage number for a^* = 15 , 8, and 4 cm. Once these resonances occur, the beam evidently continues to lose its population, the μ power decreases, and the signal phase changes. They are significant and quite fundamental problems for the multi-stage μ-source where transport of a high current beam over a long distance is indispensable to maintain a constant amount of amplified μ-power.

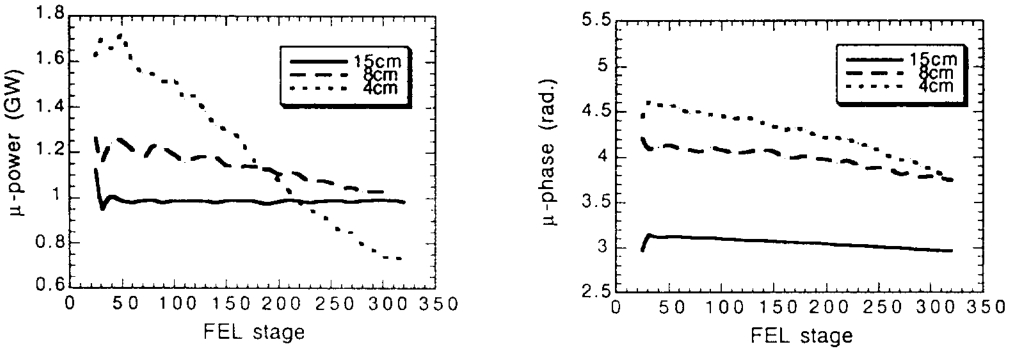

(a) (b)

Fig. 3 Evolution (simulation) of (a) m-power and (b) phase versus FEL stage number for $a^* = 15, 8, 4$ cm.

3. Nonlinear pendulum equation

In order to realize how the NR observed in the simulations occurs, we try to develop a theory based on the so-called macroparticle model discussed in several literature [7,8,9], where a bunched beam in the MFEL is treated as a single particle (macroparticle) placed at the bunch center and the amplitude and phase evolution of μ in the MFEL can be described in terms of analytic functions of the independent variable z. Following the derivation of M.L. [5] and using the definition of the macroparticle [7,8,9], the FEL equations are proved to be equivalent to the Hamiltonian

$$H(\varepsilon,\xi,E,\chi) \cong \sum_{i}^{N} \left\{ (k_w - \delta k_s)(\gamma_a + \varepsilon) + \frac{\omega_s}{2c(\gamma_a+\varepsilon)}\left(1+a_w^2\right) - a_w \left(\frac{eZ_0 J_e}{m_e c^2}\right)^{1/2} \frac{(E-N\gamma_a)^{1/2}}{N^{1/2}} \frac{\cos(\psi_a+\xi)}{\gamma_a+\varepsilon} + \frac{d\gamma_a}{dz}\xi \right\}, \tag{1}$$

where γ_a, ψ_a are the Lorentz factor and ponderomotive phase of the macroparticle, ε, ξ are deviations from the energy and phase of the macroparticle, N the number of particles, $\delta k_s = \omega_s/c - k_s$ the shift of longitudinal wavenumber from its value in vacuum, $a_w = eB_w/\sqrt{2}m_e c k_w$ the normalized wiggler amplitude, J_e beam current density, e_s normalized signal-field, e and m_e are the charge and rest mass of electron, $Z_0 = 377\Omega$, $E = Nm_e c^2 e_s^2/eZ_0 J_e$ and $\chi = -\varphi_s$. Here γ_a, ψ_a, φ_s, e_s are determined in the self-consistent FEL interaction and written in terms of the analytic functions of z according to the macroparticle model [7,8,9].

Expanding the Hamiltonian (1) in powers of ε/γ_a and retaining the dominant terms, we have the Hamiltonian

$$H(\varepsilon,\xi;z) \cong \frac{1}{2}G(z)\varepsilon^2 - F(z)\cos\psi_a \cos\xi + F(z)\sin\psi_a(\sin\xi - \xi), \tag{2}$$

where

$$G(z) = \frac{\omega_s}{c\gamma_a^3}\left(1+a_w^2\right), \quad F(z) = \frac{a_w e_s}{\gamma_a}. \tag{3a,b}$$

Neglecting friction terms which are proportional to ξ' because they are smaller than the remained terms in most of cases of our interest, a second-order differential equation

$$\xi'' + G(z)F(z)\{\sin\psi_a(\cos\xi - 1) + \cos\psi_a \sin\xi\} \approx 0, \tag{4}$$

is derived from the Hamiltonian (2), where primes denote differentiation with respect to z. Since Eq. (4) reduces to $\xi'' + G(z)F(z)\cos\psi_a\xi \approx 0$ in the limit of small amplitude oscillation ($\xi \to 0$), we can refer to Eq. (4) as a *nonlinear pendulum equation.* According to the macroparticle model [9], e_s in Eq. (3b) is written in a term of the trigonometric function

$$e_s(z) \cong \frac{2\kappa}{a|b|} \sin\frac{|b|}{2} z, \tag{5}$$

where $a \equiv \gamma_a/Ka_w k_w$, $b \equiv k_w - \delta k_s - \omega_s/2c(Kk_w a)^2$, $K \equiv eZ_0 J_e/2m_e c^2 k_w$, and $\kappa \equiv \sin\Delta\psi/\Delta\psi$ are constant which depend on the MFEL parameters [7,8]. The macroparticle model assumes $\gamma_a \propto a_w$; hence GF in Eq. (4) is determined mainly by e_s. In the limit of small-amplitude oscillation $GF\cos\psi_a$ is a periodic function of z as depicted in Fig. 4 and this linear system has been numerically proved to be stable for a parameter region of current interest although the stability of the small amplitude oscillation is not discussed in detail in this paper.

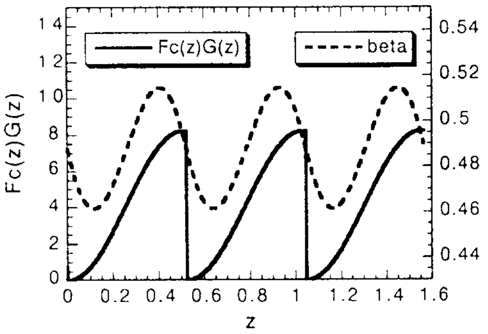

Fig. 4 The restoring coefficient $GF\cos\psi_a$ and the longitudinal amplitude function $\beta(z)$ versus the independent variable z over three periods.

Figures 5(a), (b) show the results of numerical integration of Eq. (4) in the phase space for a^* = 8, 4 cm, respectively. We observe that Eq. (4) can well reproduce the results of the FEL simulations seen in Fig. 6. Thus, we consider the Hamiltonian (1) with $E \propto e_s^2$, $\chi = -\varphi_s$ determined by the macroparticle model as a theoretical base to analytically assess the NRs in the MFEL.

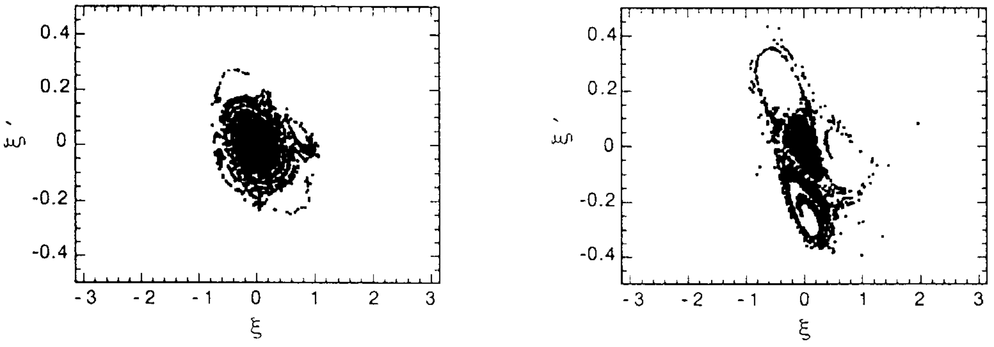

(a) (b)

Fig. 5 Phase-space plots of the nonlinear-pendulum's solution for (a) $a^* = 8$ cm and (b) $a^* = 4$ cm.

4. Isolated resonance theory

It is not difficult to calculate the size and position of the primary NR islands, using the isolated resonance theory [10] which is rather familiar in beam dynamics of circular accelerators. Expanding the Hamiltonian (1) in powers of ξ and ε/γ_a, it is written to fourth order in ξ and ε by

$$\begin{aligned} H(\varepsilon,\xi;z) &= \frac{1}{2}G\varepsilon^2 + \frac{1}{2}F_C\xi^2 - \frac{F_C}{\gamma_a^{\,2}}\varepsilon^2 - \frac{F_S}{\gamma_a}\varepsilon\xi - \frac{1}{6}F_S\xi^3 - \frac{F_C}{2\gamma_a}\xi^2\varepsilon + \frac{F_S}{\gamma_a^{\,2}}\varepsilon^2\xi \\ &\quad - \frac{1}{2}\left[G - \frac{2F_C}{\gamma_a^{\,2}}\right]\frac{\varepsilon^3}{\gamma_a} - \frac{1}{24}F_C\xi^4 + \frac{1}{6}\frac{F_S}{\gamma_a}\varepsilon\xi^3 + \frac{F_C}{2\gamma_a^{\,2}}\varepsilon^2\xi^2 - \frac{F_S}{\gamma_a^{\,3}}\varepsilon^3\xi \\ &\quad + \frac{1}{2}\left[G - \frac{2F_C}{\gamma_a^{\,2}}\right]\frac{\varepsilon^4}{\gamma_a^{\,2}}. \end{aligned} \tag{6}$$

where $F_C = F\cos\psi_a$ and $F_S = F\sin\psi_a$. The expression can be regarded as the Hamiltonian for a pendulum with time-varying "mass" G and "length" F_c, affected by nonlinear perturbations. Using the generating function $F_2(\xi,\bar{\varepsilon};z) = \xi\bar{\varepsilon}/\sqrt{G(z)}$, the Hamiltonian (6) is transformed in the form

$$H(\bar{\varepsilon},\bar{\xi};z) = 1/2\left(\bar{\varepsilon}^2 + GF_C\bar{\xi}^2\right) + (\textit{nonlinear perturbations}), \tag{7}$$

by use of the new variables $(\bar{\xi},\bar{\varepsilon})$. Furthermore we try to write the Hamiltonian in the action-angle variables (J,θ), using the generating function $F_1(\bar{\xi},\theta) = -(\alpha + \tan\theta)\bar{\xi}^2/2\beta$, where α, β satisfy

$$2\beta\beta'' - \beta'^2 + 4GF_c\beta^2 = 4, \qquad \alpha = -\beta'/2. \tag{8a,b}$$

Here β is referred to as a *longitudinal amplitude function* in the MFEL, which is a quantity analogous to a *transverse amplitude function* in circular accelerators. Since the linear part in the Hamiltonian (7) is stable or has a bounded solution, this function represents the orbital evolution of the bunch envelope in the MFEL. The periodic solution $\beta(z)$ with period L_w is uniquely determined from $G(z)F_c(z)$; a typical $\beta(z)$ calculated for parameters in Table 1 is plotted in Fig. 4. Thus the Hamiltonian (7) is transformed to

$$H(J,\theta;z) = \left(\nu_0/\beta(\mathrm{z})\right)J + (nonlinear\ perturbations). \tag{9}$$

It is convenient, for further theoretical arguments, to remove the z-dependence of the linear part. Instead of the independent variable z, we use a new variable σ defined by

$$\sigma = \frac{1}{\nu_0}\int_0^z \frac{dz'}{\beta(z')}, \qquad \nu_0 = \frac{1}{2\pi}\int_{L_w} \frac{dz'}{\beta(z')}, \tag{10a,b}$$

where $2\pi\nu_0$ is the phase advance per FEL period and ν_0 is referred to as the *longitudinal tune* or *synchrotron frequency* per period in the MFEL. Retaining only the dominant terms after some straightforward mathematical manipulation, we have the Hamiltonian written by

$$\begin{aligned} H(J,\theta;\sigma) \cong{}& \nu_0 J - \frac{1}{16}\nu_0 G^2 F_C \beta^3 J^2 + T(\theta,2\theta) \\ & - \frac{2^{3/2}}{24}\nu_0 F_S G^{3/2}\beta^{5/2}J^{3/2}\cos(3\theta) + \nu_0\frac{2^{3/2}}{8}\frac{F_C G^{1/2}}{\gamma_a}\beta^{3/2}J^{3/2}\sin(3\theta) \\ & - \frac{1}{48}\nu_0 F_C G^2\beta^3 J^2\cos(4\theta) - \nu_0\frac{1}{12}\frac{F_S G}{\gamma_a}\beta^2 J^2\sin(4\theta), \end{aligned} \tag{11}$$

where $T(\theta,2\theta)$ comprises the first and second harmonic terms of angle variable θ. Let focus on the third-integer resonance which are seen in Figs. 2(b), 5(b). The isolated resonance theory allows us to neglect all other nonresonant terms. Fourier expanding the perturbing terms

$$-\frac{2^{3/2}}{24}\nu_0 F_S G^{3/2}\beta^{5/2} = \frac{a_0}{2} + \sum_{n=1}^{\infty} a_n\cos(n\sigma) + b_n\sin(n\sigma), \tag{12a}$$

$$\nu_0\frac{2^{3/2}}{8}\frac{F_C G^{1/2}}{\gamma_a}\beta^{3/2} = \frac{c_0}{2} + \sum_{n=1}^{\infty} c_n\cos(n\sigma) + d_n\sin(n\sigma), \tag{12b}$$

substituting them into Eq. (11), and neglecting the rapidly oscillating terms, we obtain the truncated Hamiltonian

$$H_3(J,\theta;\sigma) = \nu_0\, J + h_1 J^2 + h_{31} J^{3/2}\cos(3\theta - m\sigma) + h_{32} J^{3/2}\sin(3\theta - m\sigma), \qquad (13)$$

where $h_1 \equiv -(1/2\pi)\int_0^{2\pi} \nu_0 G^2 F_C \beta^3/16 d\sigma$, $h_{31} \equiv (a_m + d_m)/2$, $h_{32} \equiv (-b_m + c_m)/2$, and m is an integer which satisfy $3\theta - m\sigma \approx 0$. To examine the phase-space structure near the resonance, we write the Hamiltonian (13) in the rotating coordinates $(\overline{J},\overline{\theta})$ obtained with the generating function $F_2(\theta,\overline{J};\sigma) = \overline{J}(\theta - m\sigma/3)$; it is just the "time"-independent Hamiltonian for the isolated third-integer resonance

$$\overline{H}_3(\overline{J},\overline{\theta}) = \delta_{m/3}\,\overline{J} + h_1\overline{J}^2 + h_3\overline{J}^{3/2}\sin(3\overline{\theta} + \Theta_3), \qquad (14)$$

where $\delta_{m/3} = \nu_0 - m/3$, $h_3 = \sqrt{h_{31}^{\ 2} + h_{32}^{\ 2}}$ and $\Theta_3 = h_{31}/h_{32}$ are constants. Using Eq. (14), the stable and unstable fixed points (SFP, UFP) of the resonance island are easily calculated from $d\overline{J}/d\sigma = -\partial\overline{H}_3/\partial\overline{\theta} = 0$, $d\overline{\theta}/d\sigma = \partial\overline{H}_3/\partial\overline{J} = 0$, then

$$\overline{J}^{1/2} = \mp\frac{3}{8}\frac{h_3}{h_1} + \left[\left(\frac{3}{8}\frac{h_3}{h_1}\right)^2 - \frac{\delta_{m/3}}{2h_1}\right]^{1/2}, \qquad (15)$$

where the upper sign means the SFP, and the lower the UFP. For simplicity we define the island width by $\Delta J \cong 2(J_{SFP} - J_{UFP})$. In a similar way, the Hamiltonian and actions at the SFP, UFP for the fourth-integer resonance islands are written by

$$\overline{H}_4(\overline{J},\overline{\theta}) = \delta_{m/4}\overline{J} + h_1\overline{J}^2 + h_4\overline{J}^2\sin(4\overline{\theta} + \Theta_4), \qquad (16)$$

$$\overline{J} = -\frac{\delta_{m/4}}{2h_1 \pm 2h_4}, \qquad (17)$$

where $-\nu_0 F_C G^2 \beta^3/48$ and $-F_S G \nu_0 \beta^2/12\gamma_a$ are Fourier expanded, $\delta_{m/4} = \nu_0 - m/4$, $h_4 = \sqrt{h_{41}^{\ 2} + h_{42}^{\ 2}}$, $\Theta_4 = h_{41}/h_{42}$, $h_{41} \equiv (a_m + d_m)/2$, $h_{42} \equiv (-b_m + c_m)/2$. Eventually we arrive at the exact mathematical formula necessary to theoretically asses the primary resonance observed in the simulations.

5. Discussion

Figs. 6(a), (b) show lines of the equi-Hamiltonian in the phase space for a^* = 8, 4 cm in the rectangular coordinates $P=\sqrt{2J}\sin\bar{\theta}$, $Q=\sqrt{2J}\cos\bar{\theta}$ to compare with the results of the simulations and the nonlinear pendulum model. A particle moves along a line because the Hamiltonians (14) and (16) are constants of motion. The position and size of the islands calculated from Eqs. (15), (17) are in agreement with simulations, as depicted in Fig. 7 where the vertical bars express the half widths of the islands obtained from simulations. The magnitude of beam-current in theoretical calculations is adjusted so as to be equal to that in the simulations with beam-loss, i.e., 1.85 kA. Thus, the resonant structure observed in the FEL simulations is identified as isolated NRs in the MFEL. In addition, Fig. 7 suggests overlapping between two different primary-resonance islands in the parameter region of small a^* (< 5 cm), in which the oscillation amplitude is well-known to quickly reach to a large size [13]. Gradual beam-loss observed in the simulations (a^* = 4 cm) can be related to this amplitude pumping mechanism.

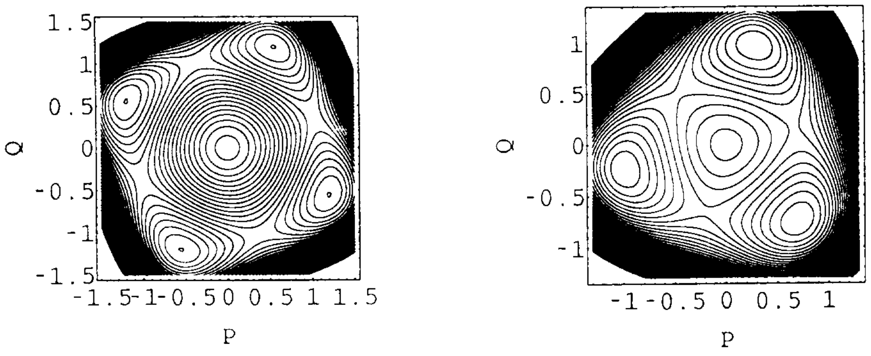

(a) (b)

Fig. 6 Phase-space plots of the equi-Hamiltonian for (a) the fourth-integer resonance (a^* = 8 cm) and (b) the third-integer resonance (a^* = 4 cm).

Shown in Fig. 8 is the longitudinal tune ν_0 calculated from Eq. (10b) as a function of a^*. The smaller the waveguide is, the larger the phase advance is. The longitudinal tune of each particle in the nonlinear system depends on its action J. We define an effective tune by $\nu=\langle\partial H_3/\partial J\rangle$, where $\langle\ \rangle$ denotes averaging with respect to phase $\bar{\theta}$. $\nu=\nu_0+2h_1J$ where h_1 is always negative in our case; therefore, the third-integer resonance occurs only when the unperturbed tune ν_0 exceeds 1/3. Also for $\nu_0>1/4$ the fourth-integer resonance can appear. Our numerical simulations certainly support this transition in the phase-space structure. Hence we can say that the longitudinal motion in the MFEL with high tune $\nu_0>1/4$ is always dominated by the large-scale lower-order NRs. In this paper, we have neglected the drift space between adjacent stages for simplicity, because simulations taking account of the drift space do not alter the qualitative features of the NRs which have been shown here.

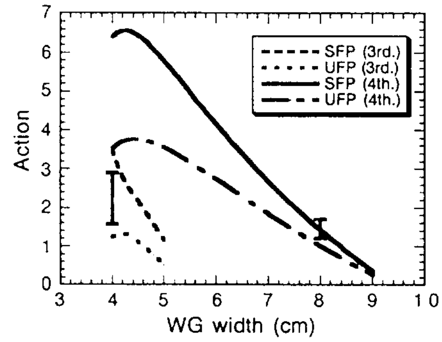

Fig. 7 Action (theoretical) of SFP, UFP versus waveguide width a^*: the third-integer resonance and the forth-integer resonance. Edges of vertical bars represent the SFP and UFP obtained by simulations.

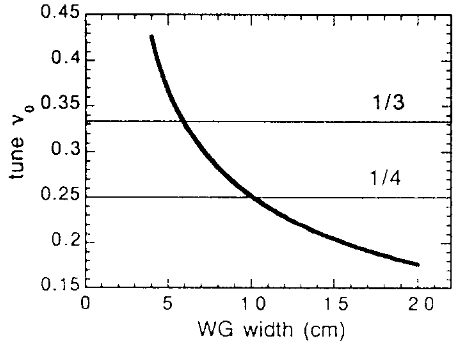

Fig. 8 Longitudinal tune ν_0 versus waveguide width a^*.

In conclusion, a theoretical model to asses the NR in the MFEL has been developed. For the first time, we have manifested the essential aspects of primary resonances by the theoretical analysis and simulations, which do determine the longitudinal phase-space structure in the MFEL. The theory is able to give a crucial suggestion in choosing practical MFEL parameters. Moreover it is noted that a concept of the NR induced by the periodicity, which is inherent in multi-stage μ-sources with an extremely large coupling between a driving beam and interaction device, will be applied to other multi-stage devices such as a relativistic klystron [14].

One of authors (S.H.) thanks Prof. Hiramatsu for useful suggestions. The numerical calculations were performed on DEC 3000 AXP-500.

References

[1] A. M. Sessler, AIP Conf. Proc. 91 (1982) 163.

[2] A. M. Sessler, E. Sternbach and J. S. Wurtele, Nucl. Inst. and Meth. B40/41 (1989) 1064.

[3] T. J. Orzechowski, B. Anderson, J. C. Clark, W. M. Fawley, A. C. Paul, D. Prosnitz, E. T. Scharlemann, S. M. Yarema, D. B. Hopkins, A. M. Sessler and J. S. Wurtele, Phys. Rev. Lett. 57 (1986) 2172

[4] K. Takayama, J. Kishiro, K. Ebihara, T. Ozaki, S. Hiramatsu and H. Katoh, J. Appl. Phys. 77 (1995) 5467

[5] N. W. Murray and M. A. Lieberman, AIP Conf. Proc. 130 (1987) 345.

[6] D. B. Hopkins, G. W. Koehler, R. W. Kuenning, W. Low, A. M. Sessler, D. Prosnitz, A. L. Throop, G. R. Westenskow and J. Haimson, Proc. IEEE Particle Accelerator Conf., IEEE Cat. no. 87CH2387-9, vol. 1. (1987) 80.

[7] K. Takayama, Phys. Rev. Lett. 63 (1989) 516.

[8] K. Takayama, Part. Accel. 39 (1992) 65.

[9] K. Takayama, R. Govil and A. M. Sessler, Nucl. Inst. and Meth. A320 (1992) 587

[10] See, for example, A. Schoch, CERN 57-21 (1958); G. Guignard, CERN 78-11 (1978).

[11] N. M. Kroll, P. L. Morton and M. N. Rosenbluth, IEEE J. Quantum Electron., QE-17 (1981) 1436.

[12] D. Prosnitz, A. Szoke, and V. K. Neil, Phys. Rev. A 24 (1981) 1436.

[13] B.V.Chirikov, Phys. Rep. 52, No.5 (1979).

[14] A. M. Sessler and S. S. Yu, Phys. Rev. Lett. 58 (1987) 2439.